

## SPECIAL FEATURES OF PROPAGATION OF PEAT FIRE

A. N. Subbotin

UDC 536.24:533.6

*The laws governing propagation of peat fire under varying outer conditions and different moisture contents are studied. Critical values of moisture content and the conditions of heat and mass exchange of a peat bed and the surrounding medium under which combustion can stop are determined based on numerical calculations. It is found that under certain conditions the combustion wave propagates along the peat bed even in the absence of air influx from the outer medium. The assumption that in small losses of heat to the outer medium the combustion wave will propagate along the bed surface and in intense heat transfer it will move into the depth of the bed is confirmed. It is shown that in combustion of a thick bed of peat layer-by-layer combustion may take place.*

**Problem Formulation.** Peat fires emerge, as a rule, after ground fire when local sites of burning (smouldering stumps, tussocks, etc.), which can ignite peat, remain on the burnt area; under certain conditions the burning site formed can move into the depth of the bed [1].

We assume that a porous round heat source (smouldering tussock), with a radius  $r_h$ , temperature  $T_h$ , and porosity  $\varphi_{5h}$ , is on the surface of a peat bed. We model the peat bed by a porous multicomponent multiphase reacting medium and assume that heat accumulated is sufficient for ignition. We study the laws governing propagation of the formed site of smouldering and the conditions of its starvation.

Let inhomogeneities be absent in the peat bed and the conditions of heat and mass exchange with both the surrounding medium and the underlying surface be the same along the corresponding surfaces. Then the physical process under consideration will possess cylindrical symmetry and, consequently, it is advisable to solve the problem in the cylindrical system of coordinates. We place the origin of the coordinates at the center of the base of the round source of ignition; we direct the  $r$  axis along the outer surface of the peat bed and the  $z$  axis from this surface into the depth of the bed. We allow for the evaporation of moisture, decomposition of peat, and heterogeneous and homogeneous reactions of oxidation of coke and carbon oxide. Then the system of equations describing the considered physical phenomenon, in contrast to [2, 3], where averaging over the bed thickness was done, has the following form:

equation of conservation of mass of the initial condensed substance

$$\rho_1 \frac{\partial \varphi_1}{\partial t} = -R_1, \quad \rho_2 \frac{\partial \varphi_2}{\partial t} = -R_{2s}, \quad \rho_3 \frac{\partial \varphi_3}{\partial t} = \gamma_3 R_1 - R_{3s}, \quad \rho_4 \frac{\partial \varphi_4}{\partial t} = \gamma_4 R_1, \quad (1)$$

$$\frac{\partial}{\partial t} (\rho_5 \varphi_5) + \frac{1}{r} \frac{\partial}{\partial r} (r \rho_5 \varphi_5 u) + \frac{\partial}{\partial z} (\rho_5 \varphi_5 v) = \gamma_5 R_1 + R_{2s} + R_{3s}; \quad (2)$$

equation of conservation of mass of oxygen, carbon oxide, and water vapor

$$\begin{aligned} \frac{\partial}{\partial t} (\rho_5 \varphi_5 c_{51}) + \frac{1}{r} \frac{\partial}{\partial r} (r \rho_5 \varphi_5 u c_{51}) + \frac{\partial}{\partial z} (\rho_5 \varphi_5 v c_{51}) = \frac{1}{r} \frac{\partial}{\partial r} \left( r \rho_5 \varphi_5 D_{51} \frac{\partial c_{51}}{\partial r} \right) + \\ + \frac{\partial}{\partial z} \left( \rho_5 \varphi_5 D_{51} \frac{\partial c_{51}}{\partial z} \right) - (M_{51}/2M_{52}) R_{52} - (M_{51}/M_3) R_{3s}, \end{aligned} \quad (3)$$

$$\begin{aligned} \frac{\partial}{\partial t}(\rho_5 \varphi_5 c_{52}) + \frac{1}{r} \frac{\partial}{\partial r}(r \rho_5 \varphi_5 u c_{52}) + \frac{\partial}{\partial z}(\rho_5 \varphi_5 v c_{52}) &= \frac{1}{r} \frac{\partial}{\partial r} \left( r \rho_5 \varphi_5 D_{52} \frac{\partial c_{52}}{\partial r} \right) + \\ &+ \frac{\partial}{\partial z} \left( \rho_5 \varphi_5 D_{52} \frac{\partial c_{52}}{\partial z} \right) + \gamma_{52} R_1 - R_{52}, \end{aligned} \quad (4)$$

$$\begin{aligned} \frac{\partial}{\partial t}(\rho_5 \varphi_5 c_{53}) + \frac{1}{r} \frac{\partial}{\partial r}(r \rho_5 \varphi_5 u c_{53}) + \frac{\partial}{\partial z}(\rho_5 \varphi_5 v c_{53}) &= \frac{1}{r} \frac{\partial}{\partial r} \left( r \rho_5 \varphi_5 D_{53} \frac{\partial c_{53}}{\partial r} \right) + \\ &+ \frac{\partial}{\partial z} \left( \rho_5 \varphi_5 D_{53} \frac{\partial c_{53}}{\partial z} \right) + \gamma_{53} R_1 - R_{2s}; \end{aligned} \quad (5)$$

equation of energy conservation

$$\begin{aligned} \sum_{j=1}^5 \rho_j \varphi_j c_{pj} \frac{\partial T}{\partial t} + \rho_5 \varphi_5 c_{p5} \left( u \frac{\partial T}{\partial r} + v \frac{\partial T}{\partial z} \right) &= \frac{1}{r} \frac{\partial}{\partial r} \left( r (\lambda + \lambda_r) \frac{\partial T}{\partial r} \right) + \\ &+ \frac{\partial}{\partial z} \left( (\lambda + \lambda_r) \frac{\partial T}{\partial z} \right) + q_{52} R_{52} + q_{3s} R_{3s} - q_{2s} R_{2s}; \end{aligned} \quad (6)$$

equation of motion in the Darcy form in the projections onto the  $r$  and  $z$  axes and equation of state

$$u = -\frac{K}{\mu} \frac{\partial p}{\partial r}, \quad v = -\frac{K}{\mu} \left( \frac{\partial p}{\partial z} - \rho_5 g \right), \quad p = \frac{\rho_5 R_5 T}{M_5}. \quad (7)$$

The following notation is introduced in Eqs. (1)–(6):

$$\begin{aligned} R_1 &= k_1 \rho_1 \varphi_1 \exp(-E_1/R_5 T), \quad R_{2s} = k_{2s} \rho_2 \varphi_2 \exp(-E_{2s}/R_5 T), \\ R_{3s} &= (M_3/M_{51}) s \rho_5 \varphi_5 c_{51} k_{3s} \varphi_3 \exp(-E_{3s}/R_5 T), \\ R_{52} &= T^{-2.25} k_{52} (c_{51} M_5/M_{51})^{0.25} (c_{52} M_5/M_{52}) \exp(-E_{52}/R_5 T). \end{aligned}$$

To close the system of equations (1)–(7) we must use the algebraic relations

$$\begin{aligned} \sum_{j=1}^5 \varphi_j &= 1, \quad \sum_{\alpha=1}^4 c_{5\alpha} = 1, \quad M_5 = \frac{1}{\sum_{\alpha=1}^4 \frac{c_{5\alpha}}{M_{5\alpha}}}, \\ c_{p5} &= \sum_{\alpha=1}^4 c_{p5\alpha} c_{5\alpha}, \quad \lambda_5 = \sum_{\alpha=1}^4 \lambda_{5\alpha} c_{5\alpha}. \end{aligned}$$

The system of equations (1)–(5) was solved under the following initial and boundary conditions:

$$t = 0: \quad \varphi_j = \varphi_{j0}, \quad j = \overline{1, 4}, \quad c_\alpha = c_{\alpha 0}, \quad \alpha = \overline{1, 3}, \quad \rho_5 = \rho_{50}, \quad T = T_0; \quad (8)$$

$$\begin{aligned}
r=0: \quad & \frac{\partial c_\alpha}{\partial r} = 0, \quad \frac{\partial p}{\partial r} = 0, \quad \frac{\partial T}{\partial r} = 0; \\
r=L: \quad & c_\alpha = c_{\alpha 0}, \quad T = T_0, \quad p = p_0;
\end{aligned} \tag{9}$$

$$\begin{aligned}
z=0: \quad & p|_{r>r_h} = p_e, \quad \left. \frac{\partial p}{\partial z} \right|_{r \leq r_h} = \rho_5 g - \frac{\mu}{K} \frac{\varphi_{5h}}{\varphi_{5s}} v_s, \quad \left. \lambda \frac{\partial T}{\partial z} \right|_{r \leq r_h} = \bar{\alpha}_h (T - T_h), \\
& \left. \lambda \frac{\partial T}{\partial z} \right|_{r > r_h} = \bar{\alpha}_e (T - T_e), \quad \left. \rho_5 \varphi_5 D_{5\alpha} \frac{\partial c_{5\alpha}}{\partial z} \right|_{r > r_h} = \beta_e (c_{5\alpha} - c_{5\alpha e}),
\end{aligned} \tag{10}$$

$$\left. \rho_5 \varphi_5 D_{5\alpha} \frac{\partial c_{5\alpha}}{\partial z} \right|_{r \leq r_h} = \beta_h (c_{5\alpha} - c_{5\alpha h});$$

$$z=h: \quad \frac{\partial p}{\partial z} = -\rho_5 g, \quad \frac{\partial c_\alpha}{\partial z} = 0, \quad \lambda_s \frac{\partial T}{\partial z} = \alpha_g (T - T_g).$$

This mathematical formulation was obtained from a general mathematical model given in [4].

**Numerical Calculations and Their Analysis.** In numerical solution of the problem, Eqs. (1)–(7) and initial (8) and boundary (9), (10) conditions were first reduced to the dimensionless form, then the components of the filtration rate were eliminated from the system by (5). Equations (1) were reduced to a system of algebraic relations by an explicit difference scheme, and the iteration-interpolation technique (IIT) was used for solutions (2)–(4) [5]. By this technique, the partial differential equations were reduced to a system of nonlinear finite-difference equations which were solved by the Newton method. The thermophysical and kinetic parameters used in numerical calculations were taken from [6–11].

As was shown in [3], the determining factors in combustion of peatland are moisture content and heat and mass exchange with the outer medium. The laws governing the formation and deepening of the fire site on the peatland were considered in [1]; therefore, here we study the process of site propagation along the peat bed and determine the conditions under which combustion may stop.

In all calculations, combustion was initiated by a cylindrical source of ignition with a radius  $r_h = 0.05$  m on the surface of the peat bed. In all cases, the temperature of the ignition source was set equal to 750 K.

We first consider propagation of the combustion wave along the bed of peat of a small degree of decomposition ( $\rho_1 = 60$  kg/m<sup>3</sup>) with a moisture content of 15%. We assume that the parameters which characterize heat and mass exchange between the peat and the outer medium and the underlying surface are:  $\alpha_g = 0.21$  W/(m<sup>2</sup>·K),  $\alpha_e = \alpha_h = 10.36$  W/(m<sup>2</sup>·K),  $\alpha_{e,w} = 0.1$  W/(m<sup>2</sup>·K), and  $\alpha_{h,w} = 0.07$  W/(m<sup>2</sup>·K). Then, as is shown by numerical calculations, in 1.2 h, a high-temperature site with a radius of 0.035 m and a depth of 0.028 m was formed under the ignition source. The temperature at the center of the site increased to about 1100 K. Then the ignition source was removed, i.e., the boundary conditions for  $r \leq r_h$  became the same as for  $r > r_h$ . In 2 h, the size of the site was doubled and the temperature at its center decreased to 890 K. By the time instant  $t = 8.23$  h, the combustion site reached the underlying surface and the temperature at the center of it became equal to 780 K. Further, the toroidal combustion wave propagated from the ignition source toward the  $r$  axis. The isotherms in the cross section of the torus by the instant of time  $t = 29.17$  h are depicted in Fig. 1. It should be noted that, in this case, the combustion wave propagates inside the peat bed. Moisture evaporates and the pyrolysis reaction partially takes place near the boundary surfaces and the oxidation reactions occur only inside the bed. This result is caused by rather intense heat exchange with the outer medium.

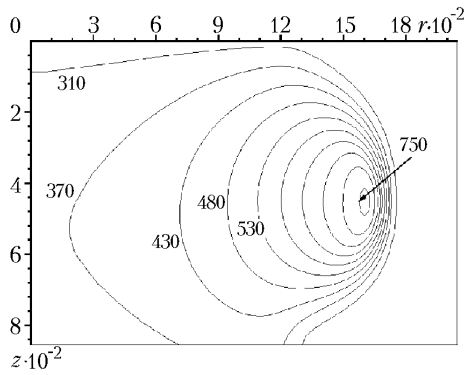


Fig. 1. Isotherms of the combustion site propagating in the bed of peat with a small degree of decomposition.  $r$ ,  $z$ , m;  $T$ , K.

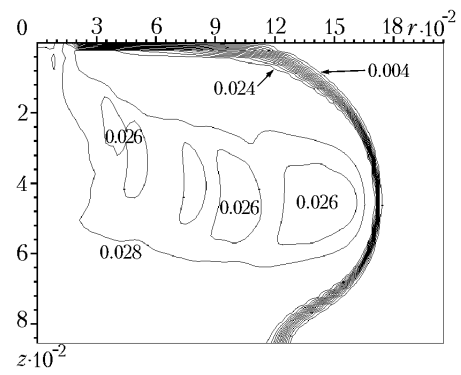


Fig. 2. Isolines of the volumetric fraction of coke formed in combustion of peat.  $r$ ,  $z$ , m.

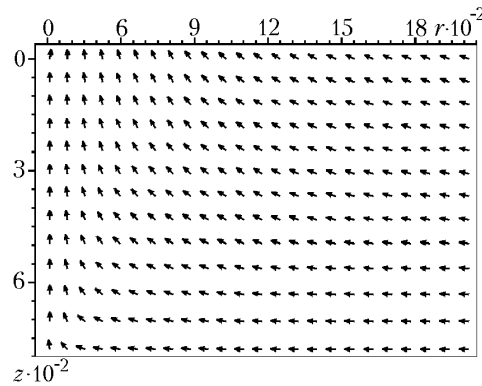


Fig. 3. Vector field of the filtration rate.  $r$ ,  $z$ , m.

Figure 2 gives the isolines of the volumetric fractions of coke formed in pyrolysis of peat for the same instant of time. As follows from the figure, the most amount of coke is formed at the center of the bed and due to the deficit of oxygen it oxidizes only partially. Pyrolysis of peat is virtually absent on the upper surface.

Figure 3 presents the vector field of the rate of filtration in peat for the same parameters and the same instant of time as in Fig. 1. Analyzing this figure, we can draw the conclusion that the gas phase moves to the center and is entrained to the outer medium through the upper surface. By virtue of the fact that the rate of filtration in the combustion zone is much larger than in the rest of the studied region, all vectors are normalized (the modulus of the vector was taken as a norm) and, therefore, the vector field in Fig. 3 shows only the direction in which the gaseous products are filtered. If we specify real relations between the velocity vectors, then beyond the combustion region they will transform to the points not showing the directions of filtration.

It should be noted that in [3], the critical moisture content was determined on the basis of a one-dimensional mathematical model. It is found that at the 100% moisture content the peat having a larger degree of decomposition does not burn. Therefore, we conducted the studies by a two-dimensional mathematical model, which were directed to determination of the critical moisture content at which the combustion of peat stops. With this in mind, ring-like bands with an increasing moisture content were set ahead of the fire front, viz., ahead of the fire front with a 15% moisture content, which propagated along peat, a ring-like band having a 30% moisture content was set, a band with a 45% moisture content followed it, and so on. Figure 4a shows the isotherms for the time instant  $t = 94.75$  h which were obtained at the same parameters and under the same conditions of heat and mass transfer as in Fig. 1 but with a moisture content increasing toward the  $r$  axis. Comparing Figs. 1 and 4a, we see that in propagation along the bed with an increasing moisture content the combustion decreases in size and the temperature in the region of the most intense oxidation increases. It should be noted that as the moisture content increases, both the site size and the rate of combustion decrease. As follows from Fig. 4b, where the isolines of the volumetric fraction of coke are presented, in tran-

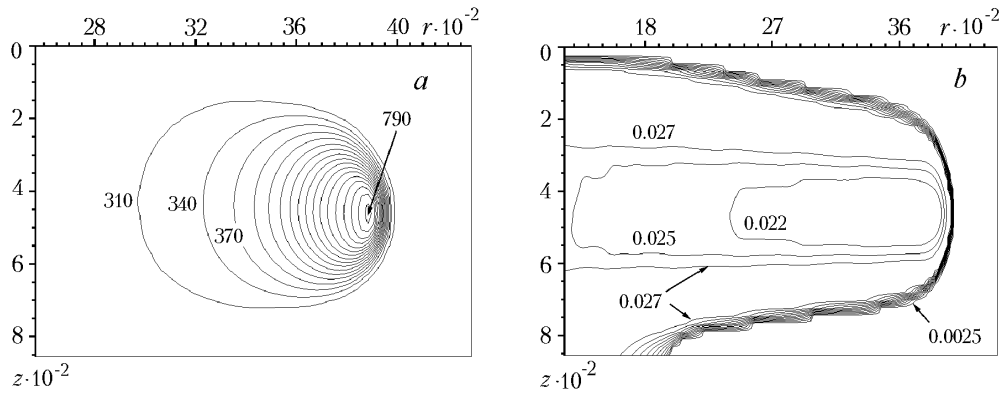


Fig. 4. Isotherms (a) and isolines of the volumetric fraction of coke (b) of the site of smouldering propagating along the bed of peat with a moisture content increasing along the radius.  $r$ ,  $z$ , m;  $T$ , K.

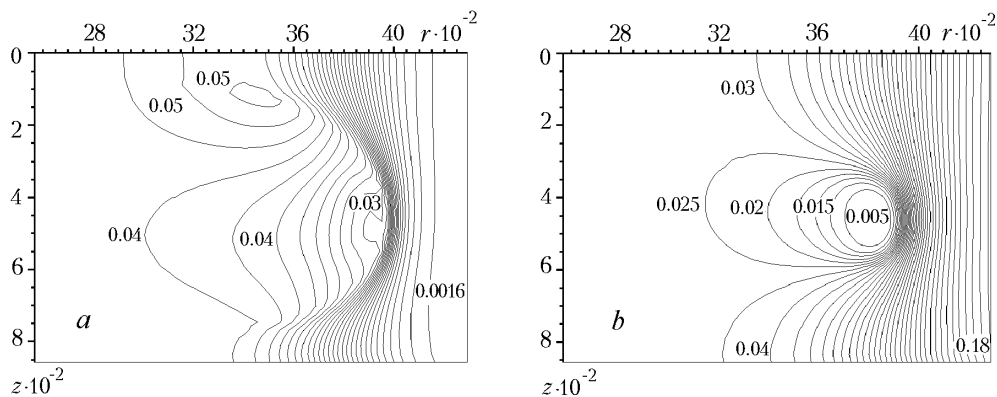


Fig. 5. Isolines of mass concentrations of water vapor (a) and oxygen (b) in the zone of combustion of the peat bed.  $r$ ,  $z$ , m.

sition to the region with a higher moisture content the size of the smouldering site decreases stepwise rather than gradually, which can be explained by the method of assignment of moisture content. Moreover, due to narrowing of the combustion region the content of oxygen in the pores of the peat per unit of the coke surface is higher, which leads to more intense oxidation of the peat. In this case, the temperature of smouldering increases (cf. Figs. 1 and 4a), thus resulting in a decrease of the volumetric fraction of coke in the burnt bed (see Figs. 2 and 4b).

In Fig. 5, the isolines of the mass concentrations of water vapor (a) and oxygen (b) are constructed for the version of calculation with an increasing moisture content. It is seen from the figures that in the burnt region the amount of water vapor is rather large and spatial distributions of mass concentration of water vapor are not symmetric relative to the peat bed. Due to free and forced convection these distributions are stretched to the center and are shifted to the upper surface of the bed. Moreover, the largest amount of water vapor is concentrated in the burnt region behind the site of smouldering. At the same time, oxygen burns virtually completely and its amount behind the combustion front is very small; therefore, the process of peat smouldering is diffusional and the rate of smouldering is fully determined by the velocity of oxygen input to the combustion site.

It was found that at the 105% moisture content, smouldering of the peat having a large degree of decomposition ( $\rho_1 = 360 \text{ kg/m}^3$ ) still proceeds, although it is strongly retarded ( $v_b = 0.2 \text{ cm/h}$ ). The peat with a 115% moisture content stops burning.

Then we studied the effect of heat and mass exchange between the peat bed and the outer medium on the laws governing propagation of the fire site. For this purpose we ignited a bed of peat with a higher degree of decomposition and a 15% moisture content. The heat and mass exchange of this bed of peat with the outer medium was determined by the parameters  $\alpha_e = 12.48 \text{ W/(m}^2 \cdot \text{K)}$ ,  $\alpha_{h,w} = \alpha_{e,w} = 0.25 \text{ W/(m}^2 \cdot \text{K)}$ , and  $\alpha_g = 0.21 \text{ W/(m}^2 \cdot \text{K)}$ . At the time instant  $t = 73.47 \text{ h}$  (3.06 days) the site of smouldering, whose size, shape, and temperature are given in Fig. 6a,

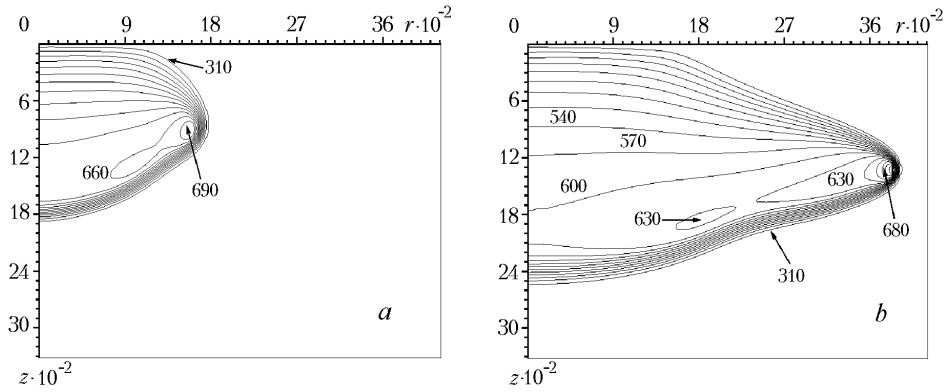


Fig. 6. Shape of the site of smouldering in peat at the instants of time  $t = 73.47$  h (a) and  $t = 160.0$  h (b) in moderate heat and mass exchange with the outer medium.  $r, z, m; T, K$ .

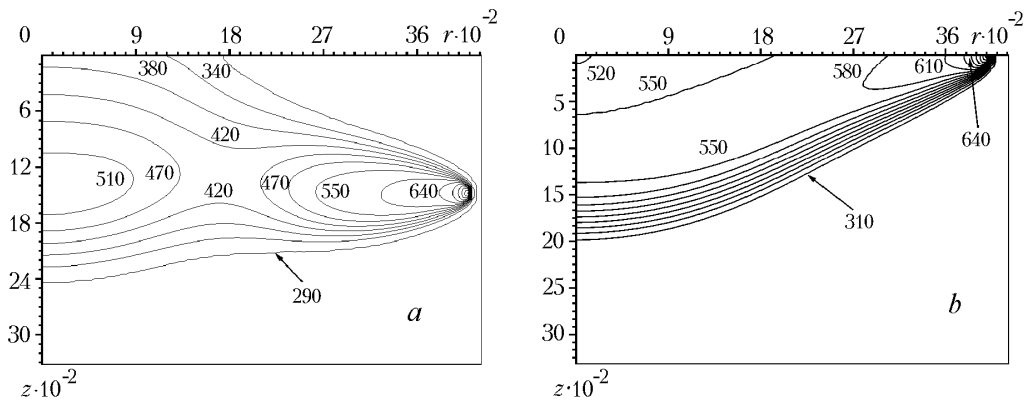


Fig. 7. Change of the shape of the site of smouldering in weak heat and mass exchange (a) and in the absence of mass exchange and very weak heat exchange with the outer medium (b).  $r, z, m; T, K$ .

was formed. On further combustion ( $t = 160.0$  h (6.67 days)), the site under consideration moved along the radius to some distance. The isotherms of this site are depicted in Fig. 6b. It is seen that under these conditions of heat and mass transfer the fire site moves into the depth and propagates toward the  $r$  axis.

We consider the case where on the upper surface of the peat bed (shown in Fig. 6a) at the time instant  $t = 73.47$  h the boundary conditions changed. Let the conditions of heat and mass transfer after the indicated instant of time be characterized by the parameters  $\alpha_e = 0.14$  W/(m<sup>2</sup>·K),  $\alpha_{h,w} = 0.07$  W/(m<sup>2</sup>·K),  $\alpha_{e,w} = 0$ , and  $\alpha_g = 0.21$  W/(m<sup>2</sup>·K), i.e., heat exchange with the near-ground layer of air decreased sharply and weak mass exchange of the gaseous products formed in the peat is exerted only through a site where the ignition source was located initially. Then, to the time instant  $t = 235.67$  h (9.82 days) the site of burning (smouldering) occupies a somewhat different place. The isotherms of this site are shown in Fig. 7a. Analyzing Figs. 6b and 7a, we can draw the conclusion that in the second case the rate of combustion decreased drastically and the region of smouldering also became smaller, but the combustion site continues to propagate inside the peat bed toward  $r$ .

Then we assume that at the time instant  $t = 73.47$  h the fire site (Fig. 6a) is covered by an impermeable, weakly heat-conducting material. In this case, the conditions of heat exchange with the outer medium are determined by the parameters  $\alpha_e = 0.014$  W/(m<sup>2</sup>·K),  $\alpha_g = 0.21$  W/(m<sup>2</sup>·K), and  $\alpha_{h,w} = \alpha_{e,w} = 0$ , which correspond to complete absence of mass transfer and very weak heat exchange of the peat bed with the outer medium. Under these conditions, the site of smouldering also continues to propagate (Fig. 7b) but the rate of smouldering becomes even smaller ( $t = 238.06$  h (9.92 days)) and the site moves toward the upper surface of the bed.

Then we considered combustion of the peat with a small degree of decomposition ( $\rho_1 = 60$  kg/m<sup>3</sup>) whose moisture content was also equal to 15%. This peat is characterized by high porosity. It was found that the rather thick

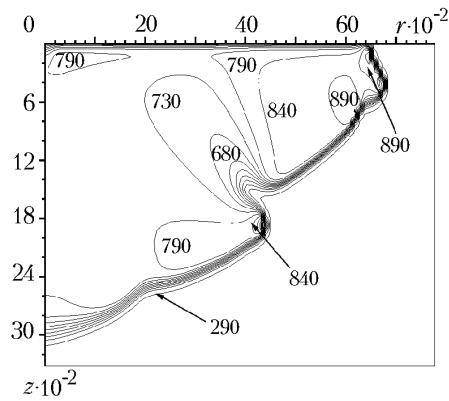


Fig. 8. Shape of isotherms in layer-by-layer combustion of peat.  $r$ ,  $z$ , m;  $T$ , K.

bed of this peat at relatively intense entrainment of the gas phase formed in the pores to the outer medium burns layer-by-layer. Thus, e.g., Fig. 8 presents the isotherms in the front of fire propagating along the bed of peat whose heat exchange with the outer medium is determined by the parameters  $\alpha_e = 0.345 \text{ W}/(\text{m}^2 \cdot \text{K})$ ,  $\alpha_{h,w} = \alpha_{e,w} = 0.138 \text{ W}/(\text{m}^2 \cdot \text{K})$ , and  $\alpha_g = 0.21 \text{ W}/(\text{m}^2 \cdot \text{K})$ . This figure is constructed for the time instant  $t = 15.89 \text{ h}$ . First, after deepening of the site, the combustion wave propagates along the upper part of the bed; then, having moved to a certain distance from the ignition source, the site of burning goes even deeper to the bed, thus forming a new combustion wave. It is noteworthy that, in this case, the rate of peat smouldering is much higher than in previous calculations. After deepening, the velocity of propagation of the site of smouldering toward the  $r$  axis became equal to about 5.2 cm/h. In previous calculations, depending on the version, it was 0.2–2.3 cm/h. The increase in the rate of combustion is caused by the relatively intense mass exchange between the peat bed and the surrounding medium, which resulted in higher ingress of oxygen into the combustion zone. An increase of mass exchange will lead to an increase on the velocity of propagation of the front of smouldering. Thus, in combustion of the 15%-moisture content peat, heat and mass exchange of which with the outer medium was determined by the parameters  $\alpha_e = 0.345 \text{ W}/(\text{m}^2 \cdot \text{K})$ ,  $\alpha_{h,w} = \alpha_{e,w} = 0.31 \text{ W}/(\text{m}^2 \cdot \text{K})$ , and  $\alpha_g = 0.21 \text{ W}/(\text{m}^2 \cdot \text{K})$ , the velocity of propagation of the leading edge of smouldering after deepening of the site was equal to 7.05 cm/h.

It should be noted that the obtained numerical results on the temperature and the rate of combustion of the peat are in agreement with the results of [12]. Here, it is shown on the basis of the field experiment that the rate of combustion of the peat with the 15% moisture content under the conditions of the experiment is 7 cm/h, and that of the peat with the 70% moisture content — 0.7 cm/h. The temperature of smouldering, according to the data of [12], varied within 623–673 K and in some cases reached 783 K.

## CONCLUSIONS

Analyzing the results of numerical calculations of the suggested mathematical model of fire propagation in the peatland, we can draw the following conclusions:

1. The considered mathematical model of the phenomenon allows determination of the site size and the velocity of propagation of the combustion wave.
2. In weak heat exchange with the outer medium, the combustion wave propagates along the surface, whereas in relatively intense heat exchange it moves into the depth of the bed.
3. It is shown that under certain conditions combustion of the peat bed continues even in the absence of mass exchange between the bed and the outer medium.
4. It is found that the limiting value of moisture content, at which peat smouldering stops, is in rather good agreement with the results obtained by a one-dimensional model [2].
5. The conditions of heat and mass transfer under which the peat burns layer-by-layer are determined.
6. On the basis of the numerical calculations made we can state that in combustion of the peat bed only the processes of drying and pyrolysis occur in full volume whereas oxidation of coke takes place partially, since the

amount of oxygen in the pores is not sufficient for complete burning of the coke formed; therefore, destruction of the upper bed of smouldering peat leads to enhancement of the process of combustion.

7. The constants for heat and mass exchange between the peat bed and the near-ground layer of air, at which the calculated rate and temperature of smouldering coincide with the data of the field experiments, are found.

8. The mathematical model suggested allows one to predict how combustion will propagate under one or another effect on the boundary of the burning peat bed and under which conditions combustion can stop.

## NOTATION

$T$ ,  $T_g$ ,  $T_e$ , and  $T_h$ , temperature of the peat bed, underlying surface, outer medium, and ignition source, K;  $h$  and  $L$ , thickness and radius of the peat bed under investigation, m;  $r_h$ , radius of the ignition source, m;  $r$ ,  $z$ , coordinate axes, m;  $t$ , time, sec;  $p$ , pressure of gaseous products in the pores, Pa;  $u$  and  $v$ , rate of filtration of gaseous products toward the coordinate axes  $r$  and  $z$ , m/sec;  $\gamma_3$ ,  $\gamma_4$ , and  $\gamma_5$ , mass fractions of coke, ash, and the gas phase formed in pyrolysis of peat;  $\lambda_r = 16\sigma T^3/s$ , coefficient of radiation heat conduction, W/(m·K);  $\sigma$ , Stefan–Boltzmann constant, W/(m<sup>2</sup>·K<sup>4</sup>);  $R_5$ , universal gas constant, J/(mole·K);  $s$ , specific surface area of pores, 1/m;  $g$ , free-fall acceleration, m/sec<sup>2</sup>;

$\lambda = \sum_{j=1}^5 \lambda_j \phi_j$ , thermal conductivity of the porous multiphase medium, W/(m·K);  $\rho_j$ ,  $c_{pj}$ ,  $\phi_j$ , and  $\lambda_j$  ( $j = 1, \dots, 5$ ), true densities, specific heat capacities, volumetric fractions, and thermal conductivities of peat, water, coke, ash, and the gas phase, respectively, kg/m<sup>3</sup>, J/(kg·K);  $c_{p5\alpha}$ ,  $\lambda_{5\alpha}$ ,  $c_{5\alpha}$  ( $\alpha = \overline{1, 3}$ ), specific heat capacities, thermal conductivities, mass concentrations of the  $\alpha$  component of the gas phase;  $D_{5\alpha}$ , effective coefficients of diffusion of the  $\alpha$  component of the gas phase, m<sup>2</sup>/sec;  $K$ , permittivity of the porous medium, according to Darcy  $k = 1.02 \cdot 10^{-12} m^2$ ;  $\mu$ , coefficient of dynamic viscosity, Pa·sec;  $R_1$  and  $R_{2s}$  and  $R_{3s}$ , mass flow rates of peat decomposition and moisture evaporation and coke oxidation, kg/(m<sup>3</sup>·sec) and kg/(m<sup>2</sup>·sec);  $M_5$ ,  $M_3$ , and  $M_{5\alpha}$  ( $\alpha = \overline{1, 3}$ ), molecular mass of the gas mixture, atomic mass of carbon, and molecular masses of oxygen, carbon oxide, and water vapor, kg/mole;  $k_{3s}$ ,  $k_{2s}$ ,  $k_1$ ,  $k_{52}$  and  $E_{3s}$ ,  $E_{2s}$ ,  $E_1$ ,  $E_{52}$ , pre-exponential factors and activation energies of heterogeneous reactions of coke combustion moisture evaporation, homogeneous reactions of peat decomposition, oxidation of carbon oxide and water vapor, m/sec; 1/sec; J/mole;  $\alpha_e$ ,  $\alpha_h$ , and  $\alpha_g$ , heat-transfer coefficients characterizing heat exchange between the peat bed and the outer medium, heat source, and underlying surface, W/(m<sup>2</sup>·K);  $v_s$ , velocity of blowing out of gaseous products from the peat bed through the upper surface, m/sec;  $v_b$ , velocity of propagation of the site of smouldering (rate of combustion), m/sec;  $q_{2s}$ ,  $q_{3s}$ , and  $q_{52}$ , thermal effects of the reactions of moisture evaporation, coke oxidation, and oxidation of carbon oxide, J/kg;  $\bar{\alpha}_e = \alpha_e [1 - k_5(\rho_5\phi_5\nu)_s]$ , heat-transfer coefficient allowing for surface porosity;  $\bar{\alpha}_h = \alpha_h [1 - k_5(\rho_5\phi_5\nu)_h]$ , heat-transfer coefficient allowing for porosity of the heat source;  $\beta_h = \bar{\alpha}_{h,w}/c_{p5}$  and  $\beta_e = \bar{\alpha}_{e,w}/c_{p5}$ , coefficients of mass exchange of the peat bed with the ignition source and the outer medium, kg/(m<sup>2</sup>·sec);  $\gamma_{52}$  and  $\gamma_{53}$ , mass fractions of oxide and dioxide of carbon formed in peat pyrolysis;  $\gamma_{52}R_1$  and  $R_{52}$ , rates of change in the mass concentration of carbon oxide due to the reactions of peat pyrolysis and oxidation of oxide;  $\gamma_{53}R_1$  and  $R_{2s}$ , mass flow rates of the formation of water vapor due to peat decomposition and evaporation of moisture from the surface of pores. Indices: e, outer medium; h, site of ignition; s, surface; b, burning; r, radiant; g, ground; 0, initial values; 1, peat; 2, water; 3, coke; 4, ash; 5, gas phase;  $5\alpha$ ,  $\alpha$  component of the gas phase ( $\alpha = \overline{1, 4}$ ); 2s, evaporation of water (from the surface of pores); 3s, oxidation of coke (reaction takes place on the surface of pores); h, w, mass exchange with the ignition site; e, w, mass exchange with the outer medium;  $5\alpha h$ ,  $\alpha$  component of the gas phase in the ignition source;  $5\alpha e$ ,  $\alpha$  component of the gas phase in the outer medium.

## REFERENCES

1. A. N. Subbotin, in: *Proc. IVth Minsk Int. Forum "Heat and Mass Transfer–MIF-2000"* [in Russian], Vol. 4, 22–26 May 2000, Minsk (2000), pp. 224–231.



2. A. N. Subbotin, in: *Mechanics of Reacting Media and Its Applications* [in Russian], Collection of Sci. Papers, Novosibirsk (1989), pp. 57–63.
3. A. N. Subbotin, *Sib. Fiz.-Tekh. Zh.*, Issue 6, 133–137 (1992).
4. A. M. Grishin, *Mathematical Modeling of Forest Fires* [in Russian], Tomsk (1981).
5. V. N. Bertsun, A. M. Grishin, and V. I. Zinchenko, *Iteration–Interpolation Method and Its Applications* [in Russian], Tomsk (1981).
6. E. S. Shchetinkov, *Physics of Gas Combustion* [in Russian], Moscow (1965).
7. V. N. Yurenev and N. D. Lebedev (eds.), *Handbook on Thermal Engineering* [in Russian], in 2 vols., Moscow (1979).
8. N. B. Vargaftik, *Handbook on Thermophysical Properties of Liquids and Gases* [in Russian], Moscow (1972).
9. V. V. Pomerantsev, K. M. Aref'ev, D. B. Ahkmedov, et al., *Principles of the Practical Theory of Combustion* [in Russian], Leningrad (1986).
10. A. A. Borisov, Ya. S. Kiselev, and V. P. Udilov, in: *Thermophysics of Forest Fires* [in Russian], Novosibirsk (1984), pp. 23–30.
11. A. M. Grishin, *Mathematical Modeling of Forest Fires and New Methods of Fighting Them* [in Russian], Novosibirsk (1992).
12. A. A. Borisov, Al. A. Borisov, and R. S. Gorelik, in: *Thermophysics of Forest Fires* [in Russian], Novosibirsk (1984), pp. 5–12.